SURFACE SUPERCONDUCTIVITY OF NIOBIUM: ONSET ON LONG-RANGE COHERENCE

Lars von Sawilski, Sara Casalbuoni and Jürgen Kötzler
Institut für Angewandte Physik und Zentrum für Mikrostrukturforschung, Universität Hamburg
Jungiusstrasse 11, D-20355 Hamburg, Germany

Abstract

We report on magnetic response measurements on Nb-cylinders with different surface treatments: as grown, buffered chemical polishing (BCP) and electrolytical polishing (EP). By increasing the field beyond H_{c2} we observe a finite critical surface current and superconducting screening up to a novel coherent surface critical field $H_{c3}^{c}(T)$, which is followed by an incoherent surface superconductivity up to the conventional surface critical field $H_{c3}(T) = rH_{c2}(T)$. The latter state is characterized by a strongly enhanced conductivity, $\sigma'(\omega)$, and by the ratio r, which depends on the surface treatment and is always larger than the classical St. James - De Gennes value, $r_{\rm GL} = 1.695$. Surprisingly, the ratio between the coherent and incoherent transition fields $H_{c3}^{c}/H_{c3} \approx 0.81$ turns out to be independent on the surface structure, suggesting some intrinsic mechanism for the onset of coherence in the sheath of width $\xi \approx \lambda$.

INTRODUCTION

The performance of superconducting cavities crucially depends on the topological and electronic structure within the microwave penetration depth. At the typical operating frequencies of 1 GHz, a surface sheath with thickness of the order of the London length is relevant, which for pure Nb is $\lambda \sim 50\,\mathrm{nm}$. Several empirical processes have been applied to smoothen the surfaces and to reduce the surface resistance, however, the underlying physical mechanisms in the relevant layer are not yet completely understood [1-5]. The main problem is set by the difficulty to explore the structure of the thin activated layer.

As a supplementary method to the existing ones [1-6], we recently suggested to investigate properties of the surface superconductivity (SSC) [6], which appears above H_{c2} and resides in a surface sheath of thickness of the order of the correlation length $\xi(T)$. Since for pure Nb, the Ginzburg-Landau (GL) parameter $\kappa = \lambda/\xi$ is of the order of one, the SSC resides in the same surface region as the microwave fields. In this contribution we introduce two novel experimental techniques which probe the superconducting critical currents and the low-frequency AC-conductivity of the surface sheath and may, therefore, serve as a possible tool to characterize the differently processed Nb-surfaces.

To this end, we study three Nb-cylinders: an as-grown crystal [7] (label A), and two polished ones [8] (C and E), which have been prepared from Nb-sheets [9] delivered for the cavity production at the TESLA facility. Some important properties of the samples are summarized in Table 1. Their surface roughness has been measured by AFM [10]. The thermodynamical and upper critical fields $H_{\rm c}$ and $H_{\rm c2}$, respectively, were extracted from magnetization isotherms $M(H,T)$ recorded by a SQUID-magnetometer ($\mathrm{MPMS_2}$, QUANTUM DESIGN) and displayed in Fig. 1a). The hysteresis loops signalize a strong flux pinning. Hence, we employ the reversible contributions to $M(H,T)$, shown in Fig. 1b), and the well known relations, $H_{\rm c}^2 = 2\int_0^{H_{\rm c2}} M_{\rm rev}\, dH$ and $M_{\rm rev}(H \nearrow H_{\rm c2}, T) = 0$, to determine the critical fields and the GL correlation lengths and κ.

Table 1: Characteristic parameters of the Nb cylinders under study.

Label	**A**	**C**	**E**
T_c (K)	9.22(1)	9.263(3)	9.263(3)
RRR	≈ 100	≈ 300	≈ 300
preparation	as grown	BCP	BCP + EP
surf. rough. (nm)	≈ 300	≈ 2	≈ 1
$H_{\rm c}(0)$ (kOe)	1.90(5)	1.80(5)	1.80(5)
$H_{\rm c2}(0)$ (kOe)	4.65(5)	4.10(5)	4.10(5)

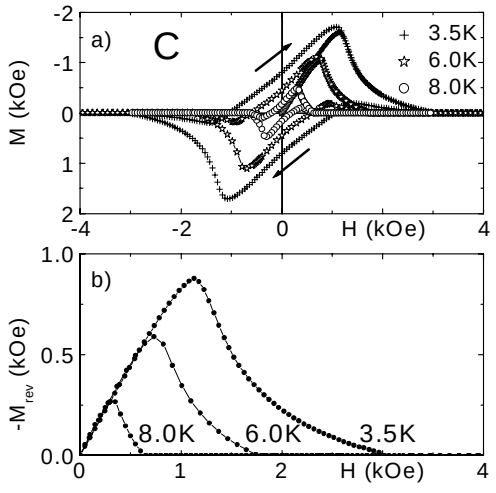

Figure 1: a) Magnetization loops measured on Nb-cylinder C at various temperatures, b) reversible magnetization, $M_{\rm rev} = (M_+ + M_-)/2$, determined from a), where M_+ and M_- are the results measured by increasing and decreasing the external field, respectively.

SURFACE CRITICAL CURRENT

We excite the surface critical current density J_c^s around the circumference of the cylinders by a gradient technique illustrated by the inset to Fig. 2, i.e. by an electric field $E_\varphi = \mu_0 \cdot (dH/dz) \cdot \dot{z}$. The scan velocity $\dot{z}$ of the sample is choosen large enough to generate the maximum surface supercurrent, $J_c^s = M - \chi H$, where χ is the contribution of the electrons in the normal conducting bulk at $H > H_{c2}$ [11]. In agreement with Lenz' rule, the sign of J_c^s depends on that of $\dot{z}$, see Fig. 2. Both existing GL-type theories [12,13] predict a power law in the reduced field difference, $h = (H_{c3}^c - H)/(H_{c3}^c - H_{c2})$

$$J_c^s(H) = J_c^s(H_{c2}) \cdot h^\beta, \qquad (1)$$

with $\beta_{GL} = 1.5$. In fact, our analyses shown in Fig. 3 reveal such behaviour, with exponents and amplitudes listed in Table 2. The larger exponents for the samples A and C can be interpreted by a larger effective dimensionality $D > 2$ of $J_c^s \sim h^{\nu(D-1)}$ [14], which may be related to the larger roughness of these samples. The magnitude of $J_c^s(H_{c2})$ is much smaller than Abrikosov's prediction for a one-current loop [12] but is rather close to the model of Ref. [13], which assumes two currents flowing on the inner and outer side of the surface sheath, $J_c^s = J_1 - J_2$.

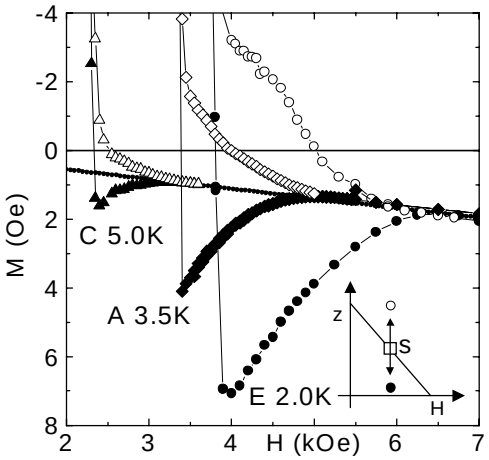

Figure 2: Magnetization above $H_{c2}(T)$ of all cylinders at the given temperatures by pulling the sample (S) antiparallel (paramagnetic peak) and parallel (diamagnetic peak) to the small gradient provided by the magnet (see inset).

SURFACE AC-CONDUCTIVITY

We determine the effective $\sigma(\omega) = \sigma' - i\sigma''$ of the cylinders from the linear AC-susceptibility using the relation [15]

$$\chi(\omega) = \chi_\infty \cdot (2I_0'(x)/(xI_0(x)) - 1)\,, \qquad (2)$$

by means of an inversion routine, where $x = (i\omega R^2 \mu_0 \sigma(\omega))^{1/2}$. For selected temperatures the $\chi(\omega)$-data are shown in Fig. 4 and the corresponding σ's in

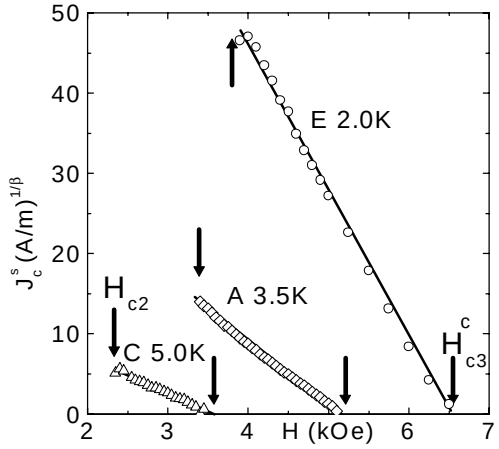

Figure 3: Power-law analysis of the magnetization peaks, $J_c^s = M - \chi H$, shown in Fig. 2, defining a surface critical field H_{c3}^c, see arrows. The exponents β are depicted in Table 2.

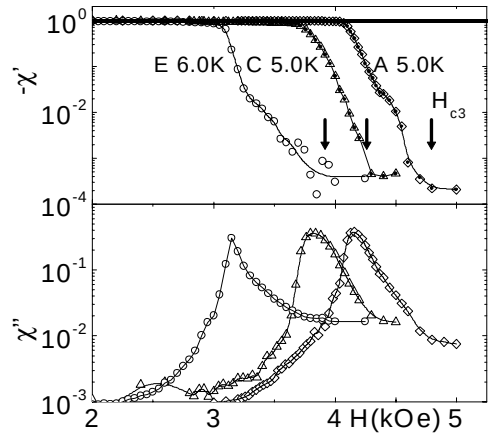

Figure 4: Field dependence of the linear AC-susceptibility above $H_{c2}(T)$ measured for all cylinders at the given temperatures and $f = 10\,\mathrm{Hz}$ using a small excitation amplitude of $10\,\mathrm{mOe}$. The arrows indicate the onset of magnetic screening at the conventional surface critical field $H_{c3}(T)$.

Fig. 5. The most prominent feature is the onset of a strong screening $\sigma''(\omega, H)$ at the same fields $H_{c3}^c(T)$, where a finite $J_c^s(H)$ arises. Approaching $H_{c3}^c(T)$ from above, we observe a strong increase of the loss component. Both parts of σ obey power laws:

$$\begin{aligned} \sigma''(H < H_{c3}^c) &= \sigma''(H_{c2}) \cdot h^\nu, \\ \sigma'(H > H_{c3}^c) &= \sigma'(H_{c2}) \cdot (-h)^{-\gamma}, \end{aligned} \qquad (3)$$

the exponents of which are also included in Table 2. The values for the electropolished sample E agree exactly with the predictions for a $2-D$ percolation transition [16], while those for A and C indicate some higher effective D, consistent with the trend of β for $J_c^s(H)$.

The other interesting feature is the onset of an excess σ and χ'' above the normal conductivity σ_n and susceptibil-

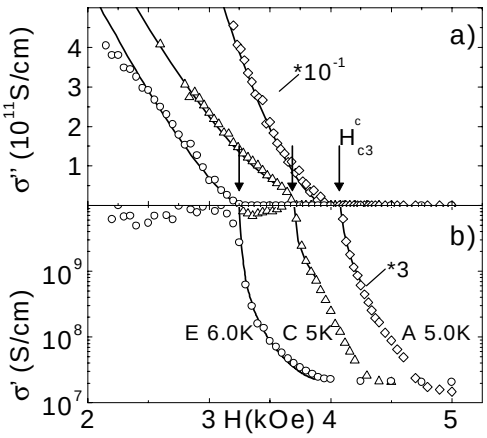

Figure 5: a) Screening and b) loss components of the linear AC-conductivity $\sigma' - i\sigma''$ extracted from $\chi' - i\chi''$, shown in Fig. 4, with the help of Eq. (3). The solid curves are fits of σ' and σ'' to Eq. (3). The exponents are indicated in Table 2.

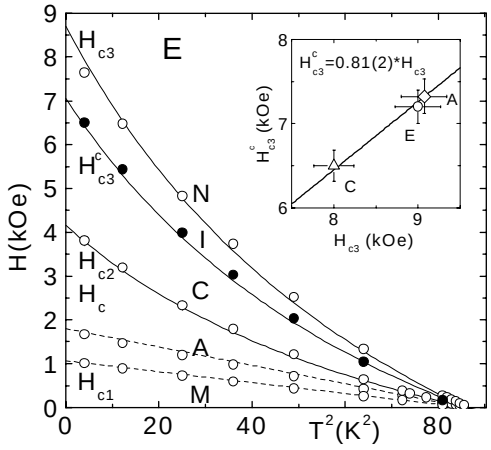

Figure 6: Temperature variation of the critical fields defining the different superconducting phases: Meissner (M), Abrikosov-Lattice (A), coherent (C) and incoherent (I) surface and normal conducting state (N), for the cylinder E. Solid curves are fits based on the empirical temperature variation of H_{c2} in Eq. (4). Inset: coherent vs. nucleation surface critical fields for all cylinders at $T = 0$.

ity $\chi''_{\rm n}$ at $H_{c3} > H^{\rm c}_{c3}$, which is commonly considered as surface critical field (indicated in Figs. 4 and 5). At H_{c3}, SSC is nucleated locally and despite a strong variation of $H_{c3}/H_{c2} = r$ (see Table 2) with surface preparation, as discussed in Ref. [6], we find the same, universal value for the ratio $H^{\rm c}_{c3}/H_{c3} = 0.81(2)$, as shown by the inset to Fig. 6.

Table 2: Critical parameters of the AC-conductivity (γ,ν) and the critical current (β) near the transition to coherent SSC (values of $J^{\rm s}_{\rm c}(H_{c2})$ in A/m).

	γ	ν	β	$J^{\rm s}_{\rm c}(H_{c2})$	r
A	1.5(1)	1.5(1)	2.1(1)	299(15)	1.70(3)
C	1.05(1)	1.4(1)	2.5(3)	88(16)	1.86(3)
E	1.3(1)	1.3(1)	1.6(1)	534(27)	2.10(3)

CONCLUSIONS

As an example, our results for the surface superconducting phases are summarized in Fig. 6 for the cylinder E along with the bulk ones. The surface phase boundaries are well explained by

$$H^{\rm c}_{c3}(T) = 0.81 \cdot H_{c3}(T) = 0.81 \cdot r \cdot H_{c2}(T), \quad (4)$$

using the well established dependence $H_{c2}(T) = H_{c2}(0) \cdot (1 - (T/T_{\rm c})^2)/(1 + (T/T_{\rm c})^2)$. Since the transition to a coherent SSC at $H^{\rm c}_{c3}$, full dots in Fig. 6, has not yet been predicted, we were not able to give quantitative interpretations of the amplitudes of the power laws for $J^{\rm s}_{\rm c}$, σ', σ'' which display significant effects of the surface treatments.

ACKNOWLEDGEMENT

We acknowledge the cooperation with E.-A. Knabbe, L. Lilje, P. Schmüser and B. Steffen (DESY, Hamburg). The work of S.C. was supported by the Deutsche Forschungsgemeinschaft through Grant No. CA 284/1-1. S.C. and L.v.S. thank the organizers for financial support.

REFERENCES

[1] P. Kneisel, Proc. 9th Works. on SRF, Santa Fe (1999)

[2] B. Aune et al., Phys. Rev. ST Accel. Beams 3, 092001 (2000)

[3] C. Antoine et al., Proc. 10th Works. on SRF, Tsukuba (2001)

[4] H. Safa, Proc. 10th Works. on SRF, Tsukuba (2001)

[5] J. Halbritter, Proc. 10th Works. on SRF, Tsukuba (2001)

[6] S. Casalbuoni et al., Proc. 11th Works. on SRF, Lübeck-Travemünde (2003)

[7] MaTecK GmbH · Im Langenbroich 20 · D-52428 Jülich · Germany

[8] L. Lilje, DESY-PhD-Thesis 2001-034 (2001); B. Steffen, DESY-Thesis 2003-014 (2003)

[9] W. C. Heraeus GmbH & Co. KG · Heraeusstrasse 12-14 · D-63450 Hanau · Germany

[10] We thank W. Gil (Hamburg) for these data.

[11] D. Hechtfischer, Z. Physik B **23**, 255 (1976)

[12] A. A. Abrikosov, Sov. Phys. JETP **20**, 480 (1965)

[13] H. J. Fink and L. J. Barnes, Phys. Rev. Lett. **15**, 792 (1965)

[14] G. Deutscher and M. Rappaport, J. Phys. Lett. **40**, L219 (1979)

[15] E. Maxwell and M. Strongin, Phys. Rev. Lett. **10**, 212 (1963)

[16] D. Stroud and D. J. Bergmann, Phys. Rev. B **25**, 2061 (1982)